

Effects of Limited Cu Supply on Soldering Reactions Between SnAgCu and Ni

C.E. HO,¹ Y.W. LIN,¹ S.C. YANG,¹ C.R. KAO,^{1,2,4} and D.S. JIANG³

1.—Department of Chemical & Materials Engineering, National Central University, Jhongli City, Taiwan. 2.—Institute of Materials Science & Engineering, National Central University, Jhongli City, Taiwan. 3.—Siliconware Precision Industries Co. 123, Sec. 3, Da Fong Road, Tanzu, Taichung, Taiwan. 4.—E-mail: kaocr@hotmail.com

The volume difference between the various types of solder joints in electronic devices can be enormous. For example, the volume difference between a 760- μm ball grid array solder joint and a 75- μm flip-chip solder joint is as high as 1000 times. Such a big difference in volume produces a pronounced solder volume effect. This volume effect on the soldering reactions between the Sn3AgxCu ($x = 0.4, 0.5, \text{ or } 0.6 \text{ wt.}\%$) solders and Ni was investigated. Three different sizes of solder spheres (300, 500, and 760 μm in diameter) were soldered onto Ni soldering pads. Both the Cu concentration and the solder volume had a strong effect on the type of the reaction products formed. In addition, $(\text{Cu,Ni})_6\text{Sn}_5$ massively spalled from the interface under certain conditions, including smaller joints and those with lower Cu concentration. We attributed the massive spalling of $(\text{Cu,Ni})_6\text{Sn}_5$ to the decrease of the available Cu in the solders. The results of this study suggest that Cu-rich SnAgCu solders can be used to prevent this massive spalling.

Key words: SnAgCu, volume effect, Cu concentration effect, Cu-Ni-Sn intermetallic, spalling

INTRODUCTION

The size of solder joints in microelectronic packages can be very different. For example, the diameter of a ball grid array (BGA) solder joint can be as large as 760 μm , and that of a flip-chip solder joint can be as small as 75 μm . Such a variation in diameter in fact translates into a 1000 times difference in volume. The so-called “solder volume effect” becomes important because of this enormous variation in volume. A number of reliability issues arise due to the volume effect as the solder joints shrink in size.^{1,2}

In BGA packages and flip-chip packages, a Ni layer is often used in the surface finishes or the under bump metallurgy (UBM) to serve as the diffusion barrier because its reaction rate with solders is about 1/100 that of Cu.³ The reactions between Ni layer and Cu-bearing solders, such as PbSnCu,^{4,5} SnAgCu,^{6–16} or SnCu solders,^{17,18} depend strongly on the Cu concentration. The well-known “Cu concentration effect” refers to the sensitivity on the Cu concentration for the reactions between Ni and Cu-bearing solders.^{15–17} As the Cu concentration

decreases from 1.0 wt.% to 0.2 wt.%, the reaction products change from single-phase $(\text{Cu,Ni})_6\text{Sn}_5$, to two-phase $(\text{Cu,Ni})_6\text{Sn}_5$ and $(\text{Ni,Cu})_3\text{Sn}_4$, and then to single-phase $(\text{Ni,Cu})_3\text{Sn}_4$. It should be noted that the above results^{15–17} were established in bulk reactions where the supply of Cu was large. In other words, the Cu concentration remained almost unchanged during soldering or during aging. In a way, the system behaves like an infinite/infinite diffusion couple. The formation of one compound or another in this case is in fact more or less dictated by thermodynamics. However, the supply of Cu is finite for a real solder joint because the solder volume is finite in real joints. Moreover, the Cu concentration in SnAgCu is almost always less than 1 wt.%. As a result, the Cu concentration in solder may change as more Cu atoms are incorporated into the reaction product(s) during soldering as well as during aging. When the Cu concentration changes, the equilibrium compound at the interface may also change. This makes the situation much more complicated. The volume effect now must be considered as the volume of solder determines the total available Cu. As the size of the joints shrink, the supply of Cu becomes more limited, and the decrease in Cu

concentration becomes more critical. The purpose of this study is to investigate the effects of limited Cu supply on the soldering reaction between SnAgCu and Ni.

EXPERIMENTAL PROCEDURES

Figure 1 shows schematically the solder joints used in this study. Solder balls of different Cu concentrations Sn₃Ag_xCu ($x = 0.4, 0.5, \text{ or } 0.6 \text{ wt.}\%$) and different diameters ($d_{\text{joint}} = 300, 500, \text{ or } 760 \text{ }\mu\text{m}$) were used to study the influence of solder volume as well as the Cu concentration. The solder volume ratio for the 300- μm , 500- μm , and 760- μm balls corresponded to 1:4.6:16.3. The contact pads have only a Ni layer over Cu (i.e., without gold). The pad opening diameter was 375 μm (i.e., $d_{\text{pad}} = 375 \text{ }\mu\text{m}$). The Ni layer was electrolytically plated.

Every substrate was first dipped into a dilute hydrochloric acid solution and then fluxed. The solder balls were placed on the pads and then reflowed for 90 sec to 1 hr at a peak reflow temperature of $235(\pm 2)^\circ\text{C}$. After soldering, the solder joints were metallographically polished to reveal the interface and the internal microstructure. In order to reveal intermetallic compounds more clearly, the polished samples were then etched with a 5 vol.% HCl (in methanol) solution for a few seconds. The thickness of the intermetallic compounds (T_{IMC}) was measured by using an image analysis software. We defined the thickness as the total area occupied by the intermetallic divided by the linear length of the interface.

The composition of reaction product(s) was identified by a JEOL JXA-8600SX electron microprobe (EPMA), operated at 20 keV. During microprobe measurement, the detected x-ray were K_{α} , K_{α} , L_{α} ,

and L_{α} for Cu, Ni, Ag, and Sn, respectively. In microprobe analysis, the concentrations of each element were measured independently, and the total weight percentage was within $100(\pm 1) \text{ wt.}\%$ in each case. For every data point, at least four measurements were made and the average value was reported.

RESULTS

Two reaction products, $(\text{Ni,Cu})_3\text{Sn}_4$ and $(\text{Cu,Ni})_6\text{Sn}_5$, were identified in this study. These two intermetallic compounds (IMCs) either formed alone or simultaneously at the interface after 90 sec to 20 min. soldering, depending on the solder volume and the Cu concentration. Table I summarizes the IMCs formed in each case. These two intermetallics, $(\text{Ni,Cu})_3\text{Sn}_4$ and $(\text{Cu,Ni})_6\text{Sn}_5$, had been established by using x-ray diffraction (XRD) in our earlier study^{15,17} to be based on the Ni_3Sn_4 and Cu_6Sn_5 structures, respectively. In the following, the results would be described in detail.

Sn₃Ag_{0.6}Cu Spheres

When a 90-sec soldering reaction between 760- μm Sn₃Ag_{0.6}Cu spheres and Ni/Cu pads took place, only a layer of $(\text{Cu,Ni})_6\text{Sn}_5$ formed at the interface, as shown in Fig. 2a. Near the reaction zone, a few $(\text{Cu,Ni})_6\text{Sn}_5$ spikes with the Ag_3Sn particles mounted in the Sn-dendrite matrix could be identified. Some of those spikes were originally connected to the $(\text{Cu,Ni})_6\text{Sn}_5$ layer through the third dimension to extend into the Sn-rich matrix. The $(\text{Cu,Ni})_6\text{Sn}_5$ at the interface existed as a needle-like layer over the Ni, which thickened to 2–3 μm thick after the reaction time was prolonged to 20 min. (Fig. 2d). Now the $(\text{Cu,Ni})_6\text{Sn}_5$ layer was thick enough to allow us to determine its composition accurately to be $(\text{Cu}_{0.64}\text{Ni}_{0.36})_6\text{Sn}_5$ at the center of the $(\text{Cu,Ni})_6\text{Sn}_5$ layer for 760- μm spheres and $(\text{Cu}_{0.60}\text{Ni}_{0.40})_6\text{Sn}_5$ for 500- μm spheres (Table I). There was no visible difference in these two $(\text{Cu,Ni})_6\text{Sn}_5$ except the size of needles. In 500- μm solder joints, the $(\text{Cu,Ni})_6\text{Sn}_5$ needles (Fig. 2b) apparently grew longer than those of the 760- μm solder joints (Fig. 2a). The mechanism for the distinct $(\text{Cu,Ni})_6\text{Sn}_5$ needles requires more-detailed study. The formation of only the $(\text{Cu,Ni})_6\text{Sn}_5$ at the interface is consistent with the results reported in the literatures,^{15,16} where the bulk reactions between Sn_{3.9}Ag_{0.6}Cu and Ni were examined.

However, the situation became radically different when a smaller solder volume was used for soldering. Figure 2c showed the results for the 90-sec reaction between a 300- μm solder sphere and Ni. The reduction in the solder volume changed the needle-like $(\text{Cu,Ni})_6\text{Sn}_5$ into a round and particle-like layer ($\sim 1.7 \text{ }\mu\text{m}$). In addition to the $(\text{Cu,Ni})_6\text{Sn}_5$ compound, a layer of a $(\text{Ni,Cu})_3\text{Sn}_4$ compound was detected within the $(\text{Cu,Ni})_6\text{Sn}_5/\text{Ni}$ interface. The presence of the $(\text{Ni,Cu})_3\text{Sn}_4$ in the 0.6 wt.% Cu-content solder joints was quite unusual considering

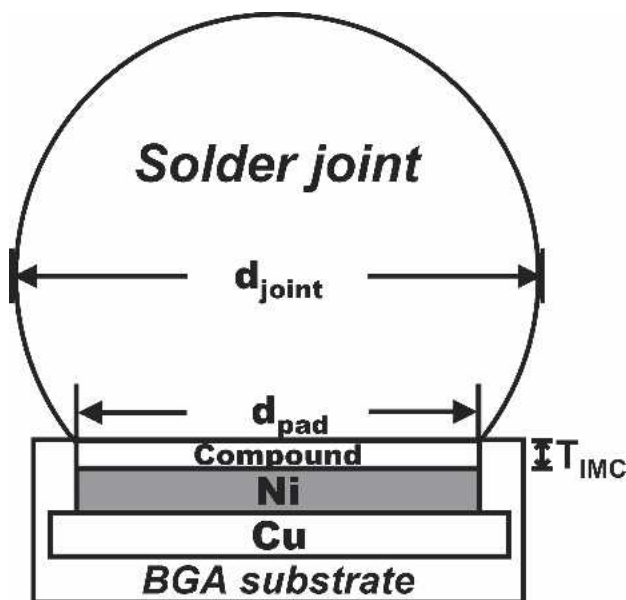


Fig. 1. Schematic diagram showing a Sn₃Ag_xCu solder sphere soldered onto a Ni/Cu pad. The parameters, d_{joint} and d_{pad} , represent the diameter of joint and pad. T_{IMC} represents the thickness of the intermetallic compound formed at the interface.

Table I. Compositions of Reaction Products in the Reaction Between Ni and Sn3AgxCu (x = 0.4–0.6 wt.%) at 235°C for 20 min.

Solder Composition (wt.%)	Reaction Product(s) with Different Ball Diameters		
	760 μm	500 μm	300 μm
Sn3Ag0.6Cu	(Cu _{0.64} Ni _{0.36}) ₆ Sn ₅	(Cu _{0.60} Ni _{0.40}) ₆ Sn ₅	(Cu _{0.59} Ni _{0.41}) ₆ Sn ₅ */(Ni _{0.79} Cu _{0.21}) ₃ Sn ₄
Sn3Ag0.5Cu	(Cu _{0.61} Ni _{0.39}) ₆ Sn ₅	(Cu _{0.56} Ni _{0.44}) ₆ Sn ₅	(Cu _{0.56} Ni _{0.44}) ₆ Sn ₅ */(Ni _{0.80} Cu _{0.20}) ₃ Sn ₄
Sn3Ag0.4Cu	(Cu _{0.58} Ni _{0.42}) ₆ Sn ₅ / (Ni _{0.80} Cu _{0.20}) ₃ Sn ₄	(Cu _{0.60} Ni _{0.40}) ₆ Sn ₅ / (Ni _{0.76} Cu _{0.24}) ₃ Sn ₄	(Cu _{0.55} Ni _{0.45}) ₆ Sn ₅ */(Ni _{0.80} Cu _{0.20}) ₃ Sn ₄

Note: The first compound listed in each entry of the table was adjacent to the solder, and the last compound was adjacent to Ni. All compounds in the table were continuous layers except those (Cu,Ni)₆Sn₅ that are marked with an asterisk (300-μm solder joints).

its growth was limited to the solders with lower Cu-content (0.5 wt.% or less).^{14–17} Moreover, a row of voids existed at the interface, separating (Cu,Ni)₆Sn₅ from (Ni,Cu)₃Sn₄ (Fig. 2c). The (Cu,Ni)₆Sn₅ intermetallics had spalled from the interface massively, allowing (Ni,Cu)₃Sn₄ to be directly exposed to solder after the reaction time reached 20 min. (Fig. 2f). Figure 3 is the zoomed-out picture of Fig. 2f. It showed that the entire layer of (Cu,Ni)₆Sn₅ had been detached from the pad, and solder was situated between (Cu,Ni)₆Sn₅ and (Ni,Cu)₃Sn₄. If the reaction time was increased further to 1 hr, the (Cu,Ni)₆Sn₅ layer would disappear from the reaction zone, as shown in Fig. 4. Now (Ni,Cu)₃Sn₄ instead of (Cu,Ni)₆Sn₅ exhibited a continuous layer at the interface. The presence of those voids in Fig. 2c could be the precursor for the detachment of (Cu,Ni)₆Sn₅ from (Ni,Cu)₃Sn₄. The underlying mechanism for the presence of (Ni,Cu)₃Sn₄ and the massive spalling of (Cu,Ni)₆Sn₅ will be explained in the Discussion.

Sn3Ag0.5Cu Spheres

As the Cu concentration slightly decreased from 0.6 to 0.5 wt.%, likewise, only a needle-like (Cu,Ni)₆Sn₅ layer formed in the larger joints (i.e., 500-μm and 760-μm-spheres) after 90 sec–20 min. of soldering (Fig. 5a, b, d, e). The compositions of the (Cu,Ni)₆Sn₅ phase did not change substantially with the adjustment of Cu concentration and were fixed at around (Cu_{0.60}Ni_{0.40})₆Sn₅ (Table I). Between Ni and (Cu,Ni)₆Sn₅, however, the (Ni,Cu)₃Sn₄ mentioned in the literatures^{11,16} was not yet observed. This was due to the (Ni,Cu)₃Sn₄ phase being either too thin to be resolved by scanning electron microscopy (SEM) or simply not present. Of course, a lower soldering temperature used in this study could be the reason. A high-resolution transmission electron microscopy study is needed to resolve this issue.

In contrast, as the solder joint diameter was reduced to 300 μm, the reaction would become different. Similar to the reaction of Sn3Ag0.6Cu (Fig.

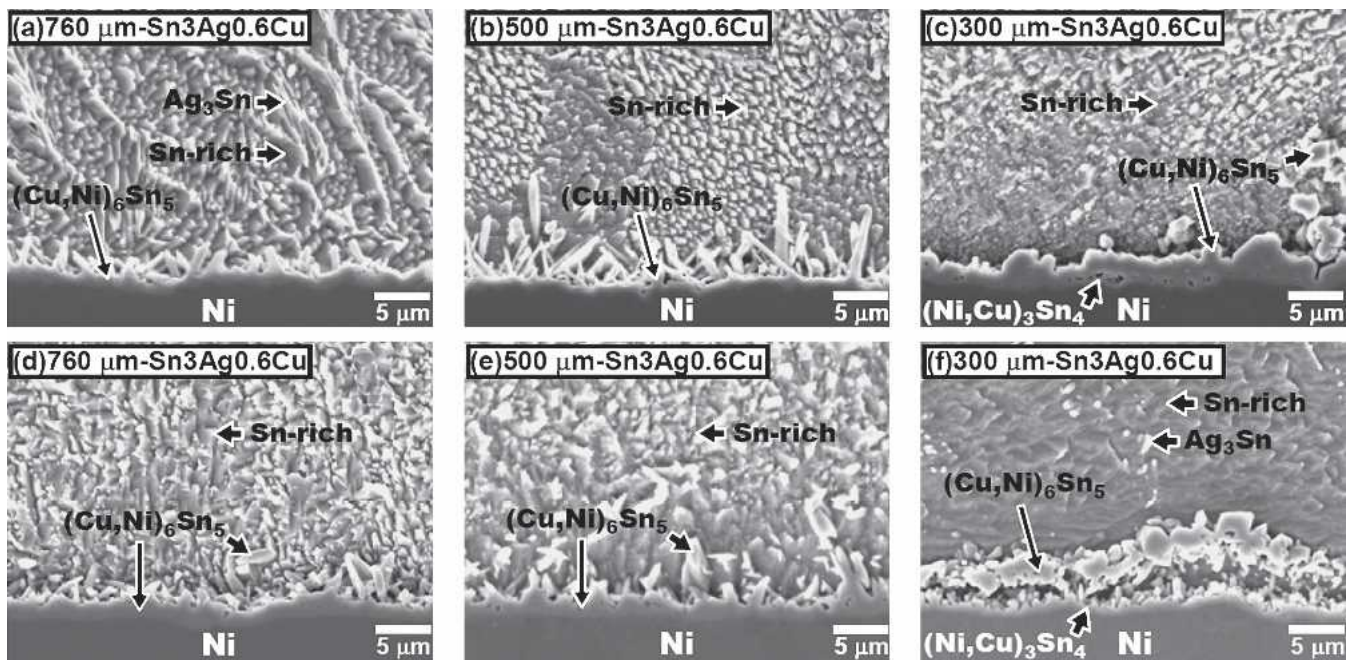


Fig. 2. Micrographs showing the interfacial reactions between Sn3Ag0.6Cu solder spheres and Ni/Cu pads after soldering for 90 sec (a–c) and 20 min. (d–f) at a peak reflow temperature of 235°C. Diameters of solder spheres were 760 μm (a, d), 500 μm (b, e), and 300 μm (c, f), respectively. The Cu layer beneath Ni was not shown in the pictures. A tin-selective etching solution (5 vol.% HCl–methanol) was used to remove part of the solder in order to reveal the morphologies of reaction zones.

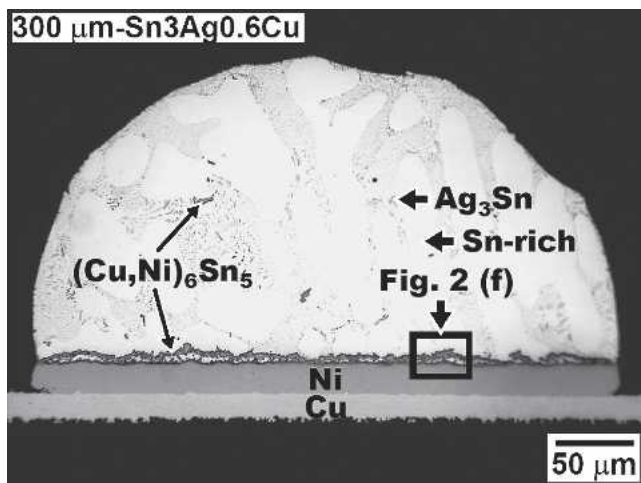


Fig. 3. Zoom-out optical micrograph of Fig. 2f. This picture was taken before acid etching was carried out.

2c), there were two intermetallics, $(\text{Cu,Ni})_6\text{Sn}_5$ over $(\text{Ni,Cu})_3\text{Sn}_4$, nucleated at the interface simultaneously (Fig. 5c). Inside the solder, some $(\text{Cu,Ni})_6\text{Sn}_5$ mixed with $(\text{Ni,Cu})_3\text{Sn}_4$ was found near the interface. As shown in Fig. 5c, the $(\text{Cu,Ni})_6\text{Sn}_5$ grains were olive-like particles with a hexagonal cross section, while the $(\text{Ni,Cu})_3\text{Sn}_4$ particles were parallelogram-shaped. The variation in the morphologies of $(\text{Cu,Ni})_6\text{Sn}_5$ and $(\text{Ni,Cu})_3\text{Sn}_4$ was attributed to the fact that they were based on different crystal structures. Above all, the results from electron microprobe showed that these particles had very similar compositions with the phases that were still attached to the interface. This evidence indicated that these particles might originate from the interface, and then spalled into the solder. When the reaction time reached 20 min., $(\text{Ni,Cu})_3\text{Sn}_4$ would replace the $(\text{Cu,Ni})_6\text{Sn}_5$ as a continuous layer, and most of the $(\text{Cu,Ni})_6\text{Sn}_5$ had left the interface (Fig. 5f), resembling the case of Sn3Ag0.6Cu/Ni (Fig. 2f) but with the amount of $(\text{Cu,Ni})_6\text{Sn}_5$ here being lower and scattered.

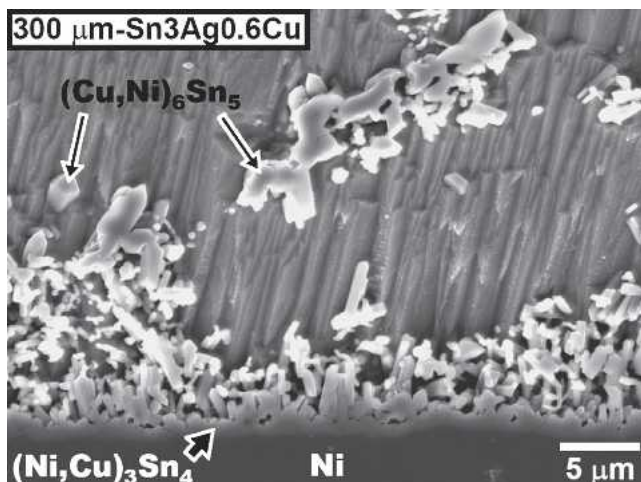


Fig. 4. Micrograph showing the interfacial reaction between a 300- μm Sn3Ag0.6Cu solder sphere and a 375- μm Ni/Cu pad after soldering for 1 hr.

Sn3Ag0.4Cu Spheres

The transition from one single $(\text{Cu,Ni})_6\text{Sn}_5$ phase to two $(\text{Cu,Ni})_6\text{Sn}_5$ - $(\text{Ni,Cu})_3\text{Sn}_4$ phases also occurred in larger solder joints, as the Cu concentration further decreased from 0.5 wt.% to 0.4 wt.%. This transitional concentration of Cu actually corresponded to the results reported in the literature¹⁶ where the supply of Cu was infinite. Shown in Fig. 6a–c are the results of Ni soldered with the Sn3Ag0.4Cu for 90 sec. Regardless of the solder volumes, interestingly, $(\text{Ni,Cu})_3\text{Sn}_4$ started to grow in all of the samples in spite of the fact that Cu concentration decreased by only 0.1 wt.%. Above the $(\text{Ni,Cu})_3\text{Sn}_4$ phase was a dense $(\text{Cu,Ni})_6\text{Sn}_5$ layer (Fig. 6a). However, the $(\text{Cu,Ni})_6\text{Sn}_5$ layer spalled into the solder when the solder balls decreased from 760 μm to 300 μm (Fig. 6a–c). Inversely, the row of voids like those mentioned in Fig. 2c increased at the interface with decreasing solder volume. As the joint shrunk to 300 μm , the underlying $(\text{Ni,Cu})_3\text{Sn}_4$ would completely replace the original $(\text{Cu,Ni})_6\text{Sn}_5$ to be in contact with solder and Ni (Fig. 6c). When the reaction time was increased to 20 min., both $(\text{Cu,Ni})_6\text{Sn}_5$ and $(\text{Ni,Cu})_3\text{Sn}_4$ would grow thicker (see Fig. 6d and e). Figure 7 was a zoom-in back-scattered electron image of the interface of Fig. 6d. It could be seen clearly that a white, wavy $(\text{Ni,Cu})_3\text{Sn}_4$ layer formed between $(\text{Cu,Ni})_6\text{Sn}_5$ and Ni. Also noted that there were some white spots like $(\text{Ni,Cu})_3\text{Sn}_4$ present within the $(\text{Cu,Ni})_6\text{Sn}_5$ layer. However, the area of these white spots was not thick enough to have their compositions determined by EPMA accurately. A further study of FE-EPMA or transmission electron microscopy (TEM) analysis is needed to clarify. As the joints shrunk to 300 μm , similarly, there was only a layer of $(\text{Ni,Cu})_3\text{Sn}_4$ with spalled $(\text{Cu,Ni})_6\text{Sn}_5$ and $(\text{Ni,Cu})_3\text{Sn}_4$ present in the reaction zone (Fig. 6f).

DISCUSSION

Cu Concentration Effect on the Soldering Reactions with Infinite Cu Supply

The “Cu concentration effect” reported in the literatures^{15–17} was established in bulk reactions where the supply of Cu approached infinity. As a result, the Cu concentration could be assumed to be constant during the study. In those studies, the interface had reached local equilibrium and the Cu-Ni-Sn isotherm¹⁹ could be used to rationalize the formation of the reaction product(s).¹⁶ For example, when the Cu concentration was high, $(\text{Cu,Ni})_6\text{Sn}_5$ was predicted to form next to the (Sn) phase due to the diffusion path would pass through the (Sn) + $(\text{Cu,Ni})_6\text{Sn}_5$ two-phase field first (point a in Fig. 8). When the Cu concentration was low, the diffusion path would pass through the (Sn) + $(\text{Ni,Cu})_3\text{Sn}_4$ two-phase field first (point b in Fig. 8), and $(\text{Ni,Cu})_3\text{Sn}_4$ was predicted to form next to the (Sn) phase. When the Cu concentration was in-between, the diffusion path would pass through the three-phase

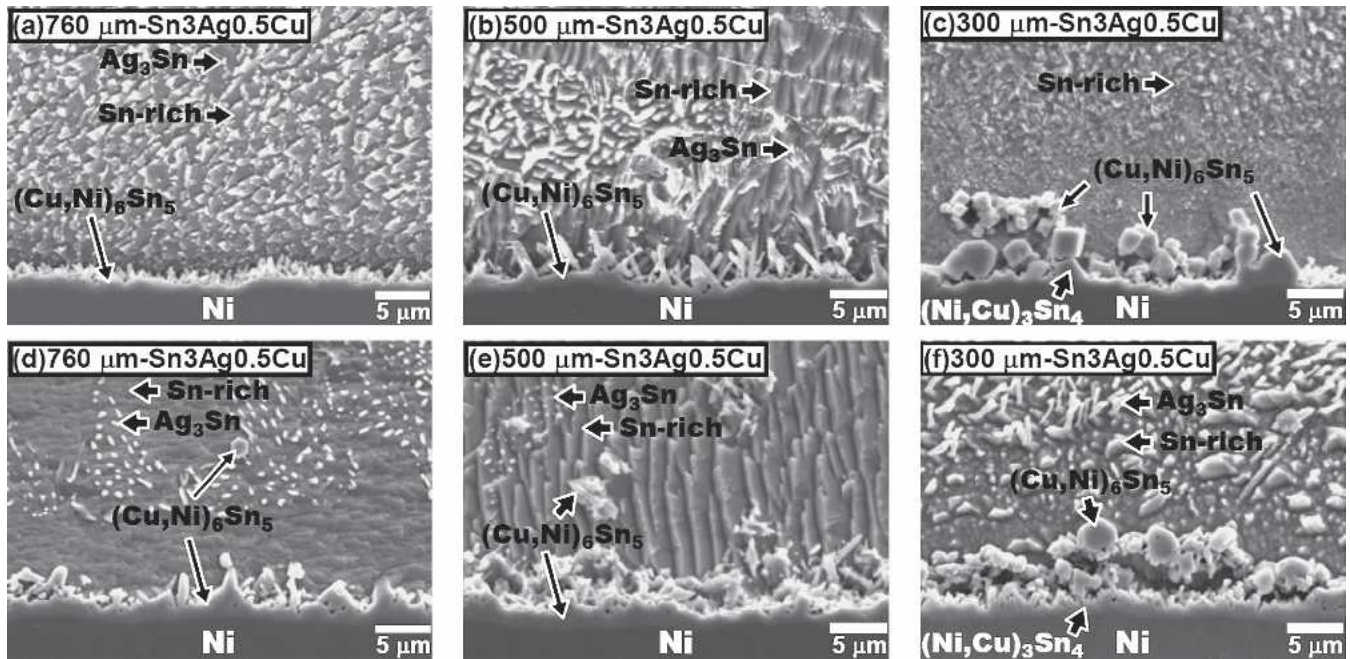


Fig. 5. Micrographs showing the results for Sn3Ag0.5Cu. All conditions are the same as their counterparts in Fig. 2.

field of (Sn) + (Cu,Ni)₆Sn₅ + (Ni,Cu)₃Sn₄ first (point c in Fig. 8), and both (Cu,Ni)₆Sn₅ and (Ni,Cu)₃Sn₄ compound formed.

In a real solder joint, the supply of Cu is limited because Cu is a minor constituent in solders. During the reaction, Cu in solder is incorporated into the reaction product(s), and as the amount of the product(s) increase, Cu in solder is gradually consumed. Consequently, the Cu concentration in solder might not be a constant during soldering, especially true for a small joint. This change in Cu concentration

then makes the reaction product at the interface change from one compound to another. As shown in the Results, this was indeed what had happened. In smaller joints, a layer of (Ni,Cu)₃Sn₄ formed at the interface despite the starting Cu concentration in the solder was as high as 0.6 wt.% (Fig. 2c and f). The term “solder volume effect” is used to describe these cases that the supply of a certain constituent is limited and affect the reaction. In the following, the relationship between the Cu concentration effect and the solder volume effect would be discussed.

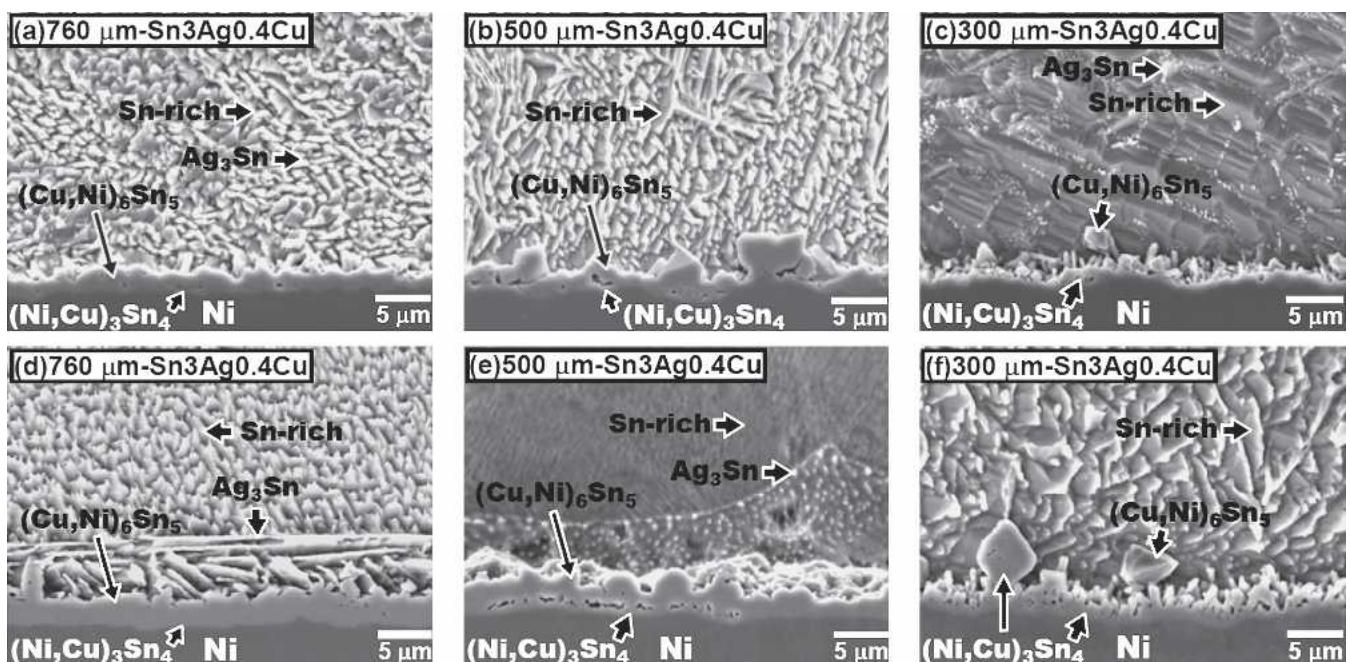


Fig. 6. Micrographs showing the results for Sn3Ag0.4Cu. All conditions are the same as their counterparts in Fig. 2.

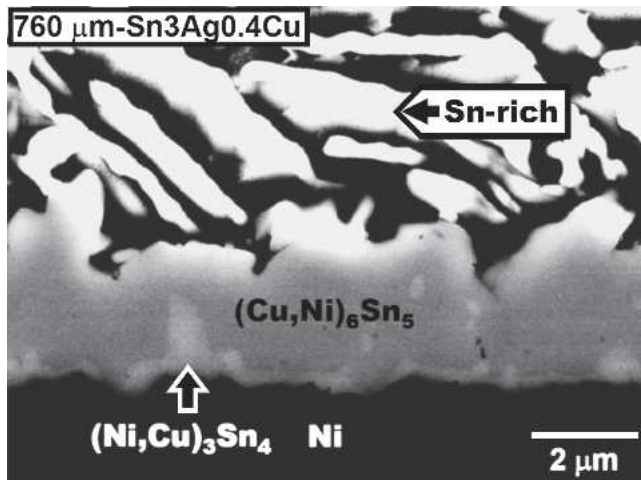


Fig. 7. Zoomed-in backscattered electron micrograph of Fig. 6d.

Effect of Limited Cu Supply

The supply of Cu in this study was limited. It decreased with the formation of Cu-bearing intermetallics, $(Cu,Ni)_6Sn_5$ and $(Ni,Cu)_3Sn_4$. The growth of these Cu-bearing intermetallics made the Cu concentration decrease to such a low level that the interfacial reaction was affected. According to the diffusion paths in the Cu-Ni-Sn isotherm (Fig. 8), this reduction in Cu concentration would change the equilibrium phase at the interface to a high degree, which destabilized the $(Cu,Ni)_6Sn_5$ layer at the interface. Consequently, $(Cu,Ni)_6Sn_5$ massively spalled from the interface. In other words, we propose that the driving force for $(Cu,Ni)_6Sn_5$ to spall massively from the interface originates from the drastic drop of Cu concentration.

In the following, let us consider the relationship between the drop of Cu concentration and the solder volume. From the mass balance of Cu, the total amount of Cu in a solder joint (Fig. 1) is equal to

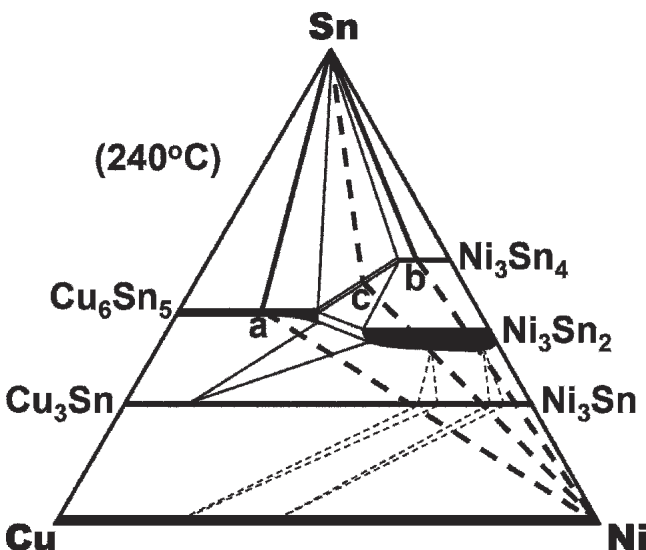


Fig. 8. Cu-Ni-Sn isotherm at 240°C. This isotherm is replotted in this study, which is adapted from Lin et al.¹⁹

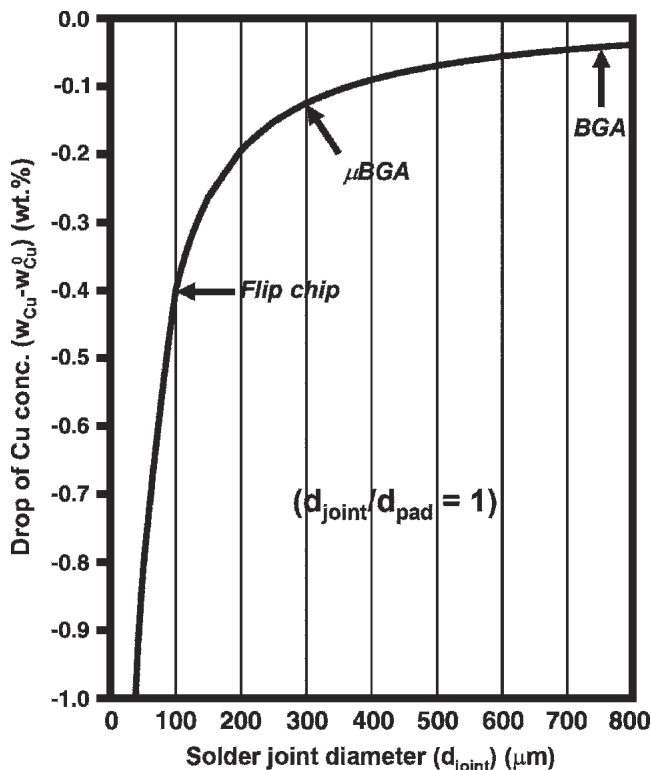


Fig. 9. Drop of the Cu concentration when 1 μ m of $(Cu_{0.60}Ni_{0.40})_6Sn_5$ formed in those joints with $(d_{joint}/d_{pad}) = 1$. This figure was calculated by using Eq. 2.

the amount of Cu in solder plus the amount of Cu in intermetallic(s). As a result,

$$\frac{4}{3} \pi \left(\frac{d_{joint}}{2} \right)^3 \rho_{solder} \cdot w_{Cu}^0 = \frac{4}{3} \pi \left(\frac{d_{joint}}{2} \right)^3 \rho_{solder} \cdot w_{Cu} + \sum_{IMC} \left[\pi \left(\frac{d_{pad}}{2} \right)^2 T_{IMC} \cdot \rho_{IMC} \cdot w_{Cu \text{ in IMC}} \right] \quad (1)$$

where w_{Cu}^0 and w_{Cu} represent the Cu concentration (wt.%) in SnAgCu before and after the soldering, respectively. The terms d_{joint} and d_{pad} represent the diameter of the solder joint and the diameter of pad's opening, respectively (see Fig. 1). The quantities ρ_{solder} and ρ_{IMC} represent the density of SnAgCu and the intermetallic, respectively. The symbol T_{IMC} represents the thickness of IMC. The densities of Sn3Ag(0.4–0.6)Cu solder spheres were determined by using a balance with 0.0001-g precision to be $\sim 7.4 \text{ g/cm}^3$. In this study, $(Cu_{0.60}Ni_{0.40})_6Sn_5$ and $(Ni_{0.80}Cu_{0.20})_3Sn_4$ were the only two Cu-bearing intermetallics that could present at the interface. The densities of Cu_6Sn_5 and Ni_3Sn_4 are 8.28 g/cm^3 and 8.65 g/cm^3 , respectively.²⁰ There are no literature values for the densities of $(Cu_{0.60}Ni_{0.40})_6Sn_5$ and $(Ni_{0.80}Cu_{0.20})_3Sn_4$. Nevertheless, Cu and Ni are immediate neighbors on the periodic table, and they have similar atomic weights and radii. Consequently, it is reasonable to approximate the densities of $(Cu_{0.60}Ni_{0.40})_6Sn_5$ and $(Ni_{0.80}Cu_{0.20})_3Sn_4$ with those of Cu_6Sn_5 and Ni_3Sn_4 .

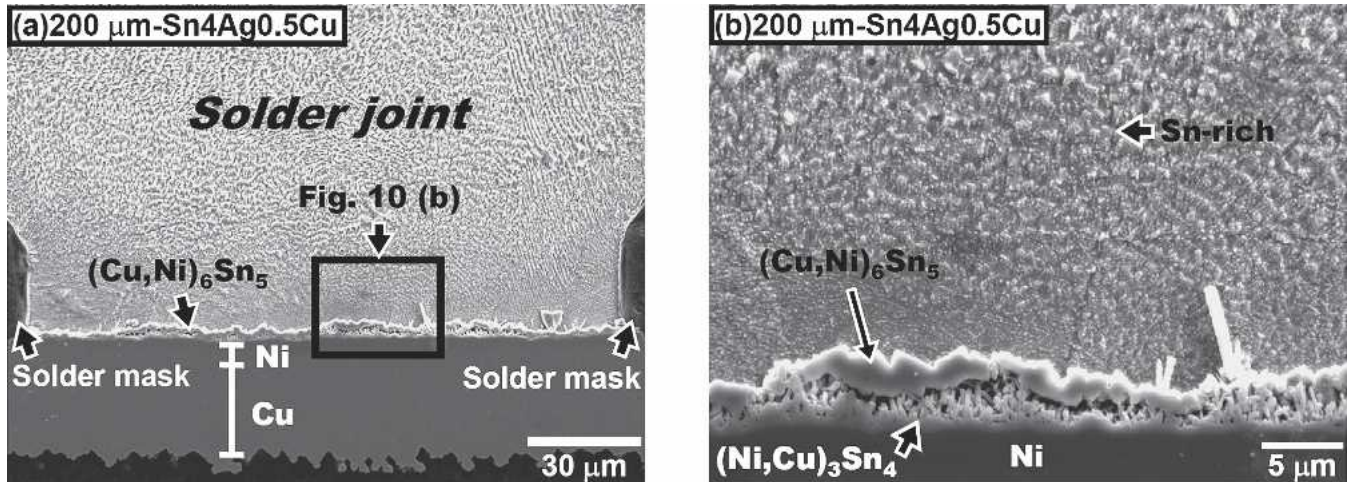


Fig. 10. (a) Flip-chip joint that produced by reflowing a 200- μm Sn4Ag0.5Cu solder sphere onto a 175- μm opening Ni/Cu pad for 90 sec at a peak temperature of 235°C. (b) Zoomed-in micrograph of (a).

For w_{Cu} in IMC, it represents the weight percentage of Cu (wt.%) in the intermetallic(s). For SnAgCu solders with Cu concentration around 0.4–0.6 wt.%, the average w_{Cu} in IMC had been determined to be 6.1 wt.% in $(\text{Ni,Cu})_3\text{Sn}_4$ and 22.7 wt.% in $(\text{Cu,Ni})_6\text{Sn}_5$. Here we have ignored those Cu in $(\text{Ni,Cu})_3\text{Sn}_4$ because the thickness of this compound was thin and its Cu concentration was low (6.1 wt.%). In other words, the second term on the right-hand side of Eq. 1 contains only the term for $(\text{Cu,Ni})_6\text{Sn}_5$. Now Eq. 1 could be simplified into the following equation,

$$w_{\text{Cu}} - w_{\text{Cu}}^0 [\text{Wt.}\%] \approx -40 \left(\frac{d_{\text{pad}}^2}{d_{\text{joint}}^3} \right) T_{(\text{Cu}_{0.60}\text{Ni}_{0.40})_6\text{Sn}_5} \quad (2)$$

According to Eq. 2, the drop of Cu concentration ($w_{\text{Cu}} - w_{\text{Cu}}^0$) under different combinations of pad diameter (d_{pad} , in μm), joint diameter (d_{joint} , in μm), and $(\text{Cu}_{0.60}\text{Ni}_{0.40})_6\text{Sn}_5$ thickness (in μm) can be calculated. From Eq. 2, we can see that the drop of the Cu concentration increases with shrinking solder joint. For example, if 2 μm of $(\text{Cu}_{0.60}\text{Ni}_{0.40})_6\text{Sn}_5$ forms in the 100 $\mu\text{m}/100 \mu\text{m}$ ball/pad combination, the Cu concentration will drop by as large as 0.8 wt.%. Under this condition, the residue Cu concentration in solder will approach zero for most commercial SnAgCu solders. Consequently, there will be a huge driving force for $(\text{Cu,Ni})_6\text{Sn}_5$ to spall in order to have a more stable $(\text{Ni,Cu})_3\text{Sn}_4$ to form at the interface. This explains why $(\text{Cu,Ni})_6\text{Sn}_5$ would tend to spall if the Cu concentration in solder is low or the solder joint is small. This also explains the observation that the presence of $(\text{Ni,Cu})_3\text{Sn}_4$ in high Cu solder joints (Fig. 2c and f).

For industry application, the ratio of the joint diameter to the pad diameter ($d_{\text{joint}}/d_{\text{pad}}$) in area-area packages is generally about 1–1.3. Flip-chip packages presently use solder joints with a diameter ranging from 200 to 75 μm , which is about 1/4 to 1/10 of current BGA solder joints (760 μm). From Eq. 2, we can see the drop of Cu concentration in

a solder joint is approximately proportional to d^{-1} , where d^{-1} is the inverse of the joint or pad diameter. As the package size continues to shrink, therefore, the drop of Cu concentration will rise rapidly. This trend can be seen in Fig. 9, where the drop of the Cu concentration was taken when 1 μm of $(\text{Cu,Ni})_6\text{Sn}_5$ formed in those joints with $(d_{\text{joint}}/d_{\text{pad}}) = 1$. In other words, the spalling of $(\text{Cu,Ni})_6\text{Sn}_5$ layer can occur more easily in smaller solder joints. Figure 10 is a cross-sectional micrograph of a 200- μm Sn4Ag0.5Cu flip-chip joint after a 90-sec soldering at 235°C. Because of its small solder volume, the $(\text{Cu,Ni})_6\text{Sn}_5$ layer was observed to spall from the $(\text{Ni,Cu})_3\text{Sn}_4$ even after one reflow.

Very recently, Jeon et al.¹¹ also reported a very similar result in 120- μm Sn4Ag0.5Cu flip-chip joints. In this study, it was observed that $(\text{Cu,Ni})_6\text{Sn}_5$ layer had been forced to spall by an additional 30 sec of soldering with the peak temperature over 300°C. Likewise, in the studies by Ghosh,^{21,22} only the $(\text{Ni,Cu})_3\text{Sn}_4$ was attached to the residue Ni/Ti when

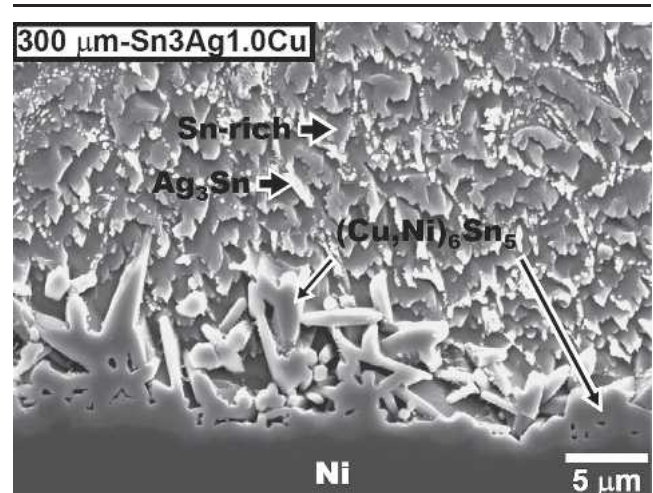


Fig. 11. Micrograph showing the interfacial reaction between a 300- μm Sn3Ag1.0Cu solder sphere and a 375- μm Ni/Cu pad after soldering for 20 min. at a peak reflow temperature of 235°C.

the Sn3Ag0.7Cu solder was soldered over a Ag (0.6 μm)/Ni (1 μm)/Ti (0.15 μm) metallization. Indeed, the fact that only (Ni,Cu)₃Sn₄ grew in such a high Cu concentration joint (Sn3Ag0.7Cu) revealed that the soldering reaction not only depended on its original Cu concentration but also on the solder volume.

Here two methods are proposed to inhibit the massive spalling. The first is to use a high Cu-bearing solder. The transition from the (Cu,Ni)₆Sn₅ compound to the (Ni,Cu)₃Sn₄ compound was indeed been delayed in the Sn3Ag1.0Cu joint with 300 μm /375 μm ball/pad combinations (Fig. 11). The second method is to provide an infinite Cu source, such as a thick Cu layer on either side of a solder joint. Our latest results also supported this view.

CONCLUSION

In the bulk reaction, the supply of Cu was infinite, and the soldering reactions between Sn-Ag-Cu and Ni strongly depend on the Cu concentration. In real joints with limited Cu supply, the reactions also depend on the solder volume. The available Cu in solder decreases as the Cu-bearing intermetallic grows. This will change the Cu concentration in solder, and consequently the equilibrium intermetallic at the interface may also change. This complication is more severe for smaller joints as less Cu is available. In the case of Cu concentration decreasing from a concentration higher than 0.4 wt.% to less than 0.4 wt.% during reflow, the (Cu,Ni)₆Sn₅ which is originally at the interface will spall massively because now the solder prefers to be in contact with (Ni,Cu)₃Sn₄.

ACKNOWLEDGEMENTS

This work was supported by the National Science Council (Grants NSC-93-2214-E-008-008 and NSC-93-2216-E-008-010). The authors thank Kinsus Inter-

connect Technology Corporation for their assistance in this study. The authors also thank Chung-Yuan Kao (National Taiwan University) for assistance in EPMA measurements.

REFERENCES

1. S.K. Kang et al., *IEEE Trans. Electron. Packag. Manuf.* 25, 155, (2002).
2. C.E. Ho, Y.W. Lin, S.C. Yang, and C.R. Kao, *Proceedings of 10th International Symposium on Advanced Packaging Materials* (Piscataway, NJ: IEEE, 2005), p. 39.
3. K. Zeng and K.N. Tu, *Mater. Sci. Eng. R* 38, 55 (2002).
4. C.E. Ho, L.C. Shiau, and C.R. Kao, *J. Electron. Mater.* 31, 1264 (2002).
5. J.H. Lee, J.H. Park, D.H. Shin, Y.H. Lee, and Y.S. Kim, *J. Electron. Mater.* 30, 1138 (2001).
6. K.Y. Lee and M. Li, *J. Electron. Mater.* 32, 906 (2003).
7. K.S. Kim, S.H. Huh, and K. Suganuma, *J. Alloys Compd.* 352, 226 (2003).
8. M.O. Alam, Y.C. Chan, and K.N. Tu, *Chem. Mater.* 15, 4340 (2003).
9. C.W. Hwang, K. Suganuma, M. Kiso, and S. Hashimoto, *J. Electron. Mater.* 10, 1200 (2004).
10. A. Sharif, M.N. Islam, and Y.C. Chan, *Mater. Sci. Eng. B* 113, 184 (2004).
11. Y.D. Jeon, K.W. Paik, A.O. Ostmann, and H. Reichl, *J. Electron. Mater.* 34, 80 (2005).
12. A. Zribi, R. Kinyanjui, P. Borgesen, L. Zavalij, and E.J. Cotts, *JOM* 54 (6), 38 (2002).
13. L.C. Shiau, C.E. Ho, and C.R. Kao, *Soldering Surf. Mount Technol.* 14, 25 (2002).
14. K. Zeng, V. Vuorinen, and J.K. Kivilahti, *IEEE Trans. Electron. Packag. Manuf.* 25, 162, 2002.
15. C.E. Ho, Y.L. Lin, and C.R. Kao, *Chem. Mater.* 14, 949 (2002).
16. C.E. Ho, R.Y. Tsai, Y.L. Lin, and C.R. Kao, *J. Electron. Mater.* 31, 584 (2002).
17. W.T. Chen, C.E. Ho, and C.R. Kao, *J. Mater. Res.* 17, 263 (2002).
18. J.S. Ha, T.S. Oh, and K.N. Tu, *J. Mater. Res.* 18, 2109 (2003).
19. C.H. Lin, S.W. Chen, and C.H. Wang, *J. Electron. Mater.* 31, 907 (2002).
20. H.P.R. Frederikse, R.J. Fields, and A. Feldman, *J. Appl. Phys.* 72, 2879 (1992).
21. G. Ghosh, *Acta Mater.* 49, 2609 (2001).
22. G. Ghosh, *J. Electron. Mater.* 33, 229 (2004).